

ESTIMATING THE NUMBER OF PEAKS IN A RANDOM FIELD USING THE HADWIGER CHARACTERISTIC OF EXCURSION SETS, WITH APPLICATIONS TO MEDICAL IMAGES¹

BY K. J. WORSLEY

McGill University

Certain three-dimensional images arising in medicine and astrophysics are modelled as a smooth random field, and experimenters are interested in the number of peaks or “hot-spots” present in such an image. This paper studies the Hadwiger characteristic of the excursion set of a random field. The excursion set is the set of points where the image exceeds a fixed threshold, and the Hadwiger characteristic, like the Euler characteristic, counts the number of connected components in the excursion set minus the number of “holes.” For high thresholds the Hadwiger characteristic is a measure of the number of peaks. The geometry of excursion sets has been studied by Adler, who defined the IG (integral geometry) characteristic of excursion sets as a multidimensional analogue of the number of “upcrossings” of the threshold by a unidimensional process. The IG characteristic equals the Euler characteristic of an excursion set provided that the set does not touch the boundary of the volume, and Adler found the expected IG characteristic for a stationary random field inside a fixed volume. Worsley, Evans, Marrett and Neelin used the IG characteristic as an estimator of the number of regions of activation of positron emission tomography (PET) images of blood flow in the brain. Unfortunately the IG characteristic is only defined on intervals: it is not invariant under rotations and it can fail to count connected regions that touch the boundary. This is important since activation often occurs in the cortical regions near the boundary of the brain. In this paper we study the Hadwiger characteristic, which is defined on arbitrary sets, is invariant under rotations and does count connected regions whether they touch the boundary or not. Our main result is a simple expression for the expected Hadwiger characteristic for an isotropic stationary random field in two and three dimensions and on a smooth surface embedded in three dimensions. Results are applied to PET studies of pain perception and word recognition.

1. Introduction. Many studies of brain function with positron emission tomography (PET) involve the interpretation of subtracted PET images, usually the difference between two three-dimensional images of cerebral blood flow under baseline and stimulation conditions. The purpose of these

Received June 1993; revised June 1994.

¹Research supported by the Natural Sciences and Engineering Research Council of Canada, and the Fonds pour la Formation des Chercheurs et l'Aide à la Recherche de Québec.

AMS 1991 subject classifications. Primary 60G60, 62M40; secondary 52A22, 92C55.

Key words and phrases. Euler characteristic, integral geometry, stereology, geometric probability, image analysis.

studies is to see which areas of the brain show an increase in blood flow, or "activation," due to the stimulation condition. The experiment is repeated on several subjects, and the subtracted images are averaged to improve the signal-to-noise ratio. The averaged image is standardized to have unit variance and then searched for local maxima, which might indicate points in the brain that are activated by the stimulus. An example of such an image is shown in Figure 1 and a more detailed explanation is given in Section 6. The main statistical problem has been to assess the significance of these local maxima.

Worsley, Evans, Marrett and Neelin (1992, 1993) have shown that the averaged image can be modelled as a Gaussian random field with a covariance function depending on the known resolution of the PET camera. The maximum of the random field was used to test for activation at an unknown point in PET images, and the IG (integral geometry) characteristic of excursion sets was used to estimate the number of regions of activation. The excursion set inside a fixed set C is just the set of points where the field exceeds a fixed threshold value. The IG characteristic of Adler (1981) equals the Euler characteristic of an excursion set provided that the set does not touch the boundary of C , and so it counts the number of connected components minus the number of "holes." The number of regions of activation is estimated using the IG characteristic for a high threshold, chosen so that if no activation is present, the expected IG characteristic equals a small value $\alpha = 0.1$, say.

Similar problems arise in astrophysics. In a series of 19 papers, starting with Gott, Mellot and Dickinson (1986) and ending most recently with Rhoads, Gott and Postman (1994), methods similar to those discussed in this paper have been used to study the density of matter in the universe. Torres (1994) has used similar tools to study the fluctuations in the cosmic microwave background which were recently discovered by Smoot et al. (1992).

Unfortunately the IG characteristic is only defined on intervals: it is not invariant under rotations and it can fail to count connected regions that touch the boundary. This is important since activation in cognitive experiments often occurs in the cortical regions near the boundary of the brain. The Hadwiger characteristic, which is defined on arbitrary sets, is invariant under rotations and does count connected regions whether they touch the boundary or not, should provide a better estimator of the number of regions of activation. The purpose of this paper is to extend the work of Adler (1981) to derive the expected Hadwiger characteristic of the excursion set of a random field. In Section 2 we define and compare the different excursion characteristics. In Section 3 we shall derive results in two dimensions and in Section 4 we shall derive results in three dimensions. Alternative derivations are presented in Section 5, based on the kinematic fundamental formula of integral geometry, and another derivation for small convex sets based on a linear approximation to the field. In Section 6 we shall apply this work to some PET images from studies in pain perception and word recognition.

This work has been extended in several ways. For C an interval, Worsley,

Evans, Marrett and Neelin (1993) find the expectation of the IG characteristic in three dimensions when the mean of the random field is nonzero. This makes it possible to find the exact bias of the Hadwiger characteristic as an estimator of the number of peaks. Siegmund and Worsley (1995) consider the problem of detecting a peak with an unknown scale as well as an unknown location. Worsley (1994a) gives results for χ^2 , F and t fields, and Worsley (1994b) uses Morse theory to generalise the present work to an arbitrary number of dimensions, provided C has a smooth boundary.

2. Excursion set characteristics. Let $X(\mathbf{t})$, $\mathbf{t} = (t_1, \dots, t_N) \in \mathbb{R}^N$, be a stationary random field in N dimensions and let C be a compact subset of \mathbb{R}^N . Two examples in three dimensions are shown in Figure 1. We define the excursion set A_b of $X(\mathbf{t})$ above a threshold b to be the set of points in C where $X(\mathbf{t})$ exceeds b :

$$A_b = \{\mathbf{t} \in C: X(\mathbf{t}) \geq b\}.$$

Adler (1981) considers two different characteristics of an excursion set: the DT (differential topology) characteristic and the IG (integral geometry) characteristic. Both characteristics equal the Euler characteristic of the excursion set when the set does not touch the boundary of C . When the set does touch the boundary, as inevitably happens for a random field, then the characteristics can differ, depending on the way in which the set touches the boundary and its orientation. Thus even though the Euler characteristic is invariant under translations, rotations or indeed any elastic deformation of Euclidean space, the same is not in general true of the DT and IG characteristics, as illustrated in Figure 2. Nevertheless, as Adler (1981) shows, both characteristics have the same expectation, which is invariant under translations and rotations. Worsley, Evans, Marrett and Neelin (1993) show that their expectations do differ when the field is nonstationary. The precise definitions of the characteristics are as follows, and illustrations are shown in Figure 2.

2.1. Definition of the DT characteristic. The DT characteristic is defined on arbitrary compact sets $C \subset \mathbb{R}^N$ directly from the field $X(\mathbf{t})$, provided that $X(\mathbf{t})$ is suitably regular as defined by Adler [(1981), Chapter 3]. These conditions ensure that the derivatives of $X(\mathbf{t})$ up to second order exist with probability 1. Let $X = X(\mathbf{t})$, $X_j = X_j(\mathbf{t}) = \partial X / \partial t_j$ and $X_{jk} = X_{jk}(\mathbf{t}) = \partial^2 X / \partial t_j \partial t_k$, $j, k = 1, \dots, N$. Let $\mathbf{D}_{N-1} = \mathbf{D}_{N-1}(\mathbf{t})$ be the $(N-1) \times (N-1)$ matrix of second-order partial derivatives of $X(\mathbf{t})$, with (j, k) element $X_{jk}(\mathbf{t})$, $j, k = 1, \dots, N-1$. The DT characteristic is defined by Adler [(1981), Section 4.4] as

$$\chi_{\text{DT}}(b) = (-1)^{N-1} \sum_{l=0}^{N-1} (-1)^l \nu_l(b),$$

where $\nu_l(b)$ is the number of points $\mathbf{t} \in C$ satisfying the conditions: (a) $X(\mathbf{t}) = b$, (b) $X_1(\mathbf{t}) = 0, \dots, X_{N-1}(\mathbf{t}) = 0$, (c) $X_N(\mathbf{t}) > 0$ and (d) the number of negative eigenvalues of $\mathbf{D}_{N-1}(\mathbf{t})$ is exactly l . An equivalent definition, written

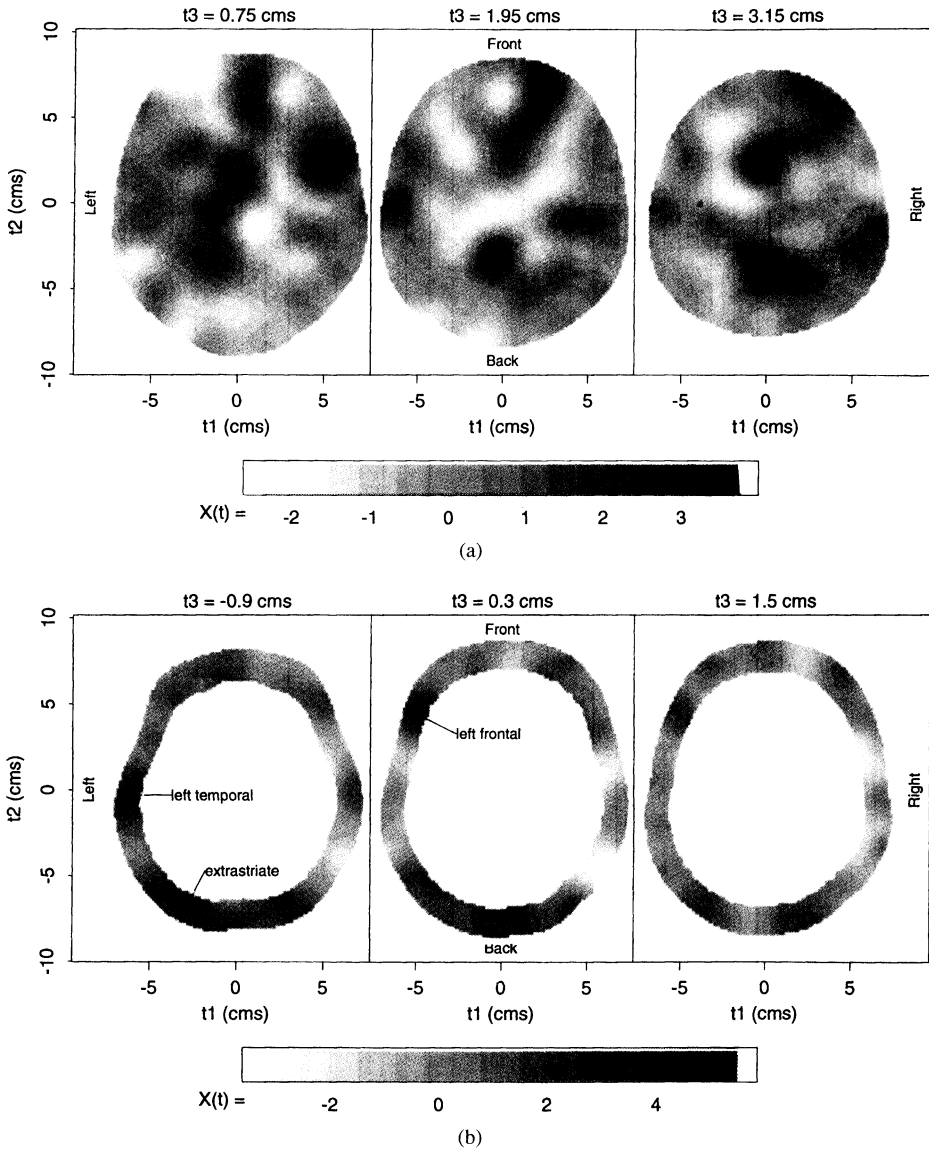


FIG. 1. An illustration of a random field in \mathbb{R}^3 . Three horizontal slices through the set C for (a) the pain study (Section 6.3) and (b) the word recognition study (Section 6.4). For the pain study, C covered the top half of the brain. For the word recognition study, C was restricted to a thin shell covering the outer cortex of the brain. The average blood flow difference across the subjects, divided by its estimated standard deviation, $X(t)$, is shown inside C ; high values are more darkly shaded, as shown on the legend below the art. No activation was expected for the pain study, but three areas of activation were identified in the word recognition study (arrows).

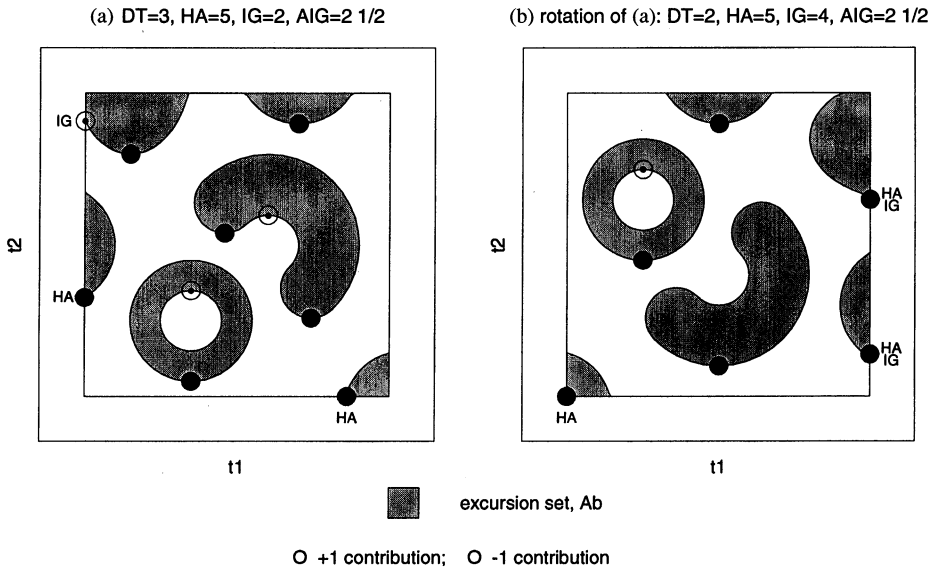


FIG. 2. Illustrations of excursion set characteristics in \mathbb{R}^2 for C an interval. Interior points contribute to all characteristics. On the boundary there are no contributions to the DT characteristic, but those points marked HA contribute to the Hadwiger characteristic and those points marked IG contribute to the IG characteristic. The AIG characteristic is the average of the IG characteristic for all reflections of the coordinate axes. Note that the DT and IG characteristics are not invariant under rotations.

as a sum over all $\mathbf{t} \in C$, is often more useful. Using the notation advocated by Knuth (1992), where a logical expression in parentheses takes the value 1 if the expression is true and 0, otherwise, we can write

$$\chi_{DT}(b) = \sum_{\mathbf{t} \in C} (X = b)(X_1 = 0) \cdots (X_{N-1} = 0)(X_N > 0) \text{sign}[\det(-\mathbf{D}_{N-1})].$$

Examples in two dimensions of the points that contribute to the DT characteristic, together with their contributions, are shown in Figure 2, where the DT characteristic is

$$\chi_{DT}(b) = \sum_{\mathbf{t} \in C} (X = b)(X_1 = 0)(X_2 > 0)[(X_{11} < 0) - (X_{11} > 0)].$$

Note that the summation is nonzero only for points where the contour $X = b$ has a tangent in the t_1 direction ($X_1 = 0$) and the excursion set is on the upper (increasing t_2) side of the contour ($X_2 > 0$). Contributions to the summation are +1 if the excursion set is convex ($X_{11} < 0$) or -1 if the excursion set is concave ($X_{11} > 0$).

2.2. Definition of the Hadwiger characteristic. Hadwiger (1959) defines the Hadwiger characteristic $\psi(A)$ iteratively for a large class of sets A called basic complexes. A compact subset B of \mathbb{R}^N is called a basic if the intersec-

tions of all k -planes with B are simply connected, $k = 1, \dots, N$. A set A is a *basic complex* if it can be represented as the union of a finite number of basics such that the intersection of any of these is again a basic [see Adler (1981), page 71].

For $N = 1$, Let $\psi(A)$ be the number of disjoint intervals in A . For $N > 1$, let

$$(2.1) \quad \psi(A) = \sum_u \{\psi(A \cap \mathcal{E}_u) - \psi(A \cap \mathcal{E}_{u-})\},$$

where $\mathcal{E}_u = \{t \in C: t_N = u\}$ and

$$\psi(A \cap \mathcal{E}_{u-}) = \lim_{v \uparrow u} \psi(A \cap \mathcal{E}_v).$$

The Hadwiger characteristic is the only characteristic which satisfies the following additivity property: If $A, B, A \cup B$ and $A \cap B$ are basic complexes, then

$$(2.2) \quad \chi(A \cup B) = \psi(A) + \psi(B) - \psi(A \cap B).$$

If $X(t)$ is sufficiently regular, as defined by Adler [(1981), Chapter 3], then the excursion set A_b is almost surely a basic complex. The Hadwiger characteristic is then defined as

$$\chi_{HA}(b) = \psi(A_b).$$

2.3. Definition of the IG characteristic. The IG characteristic is based on the Hadwiger characteristic [Adler (1981), Section 4.2]. It is defined only on an interval, which without loss of generality we can take as $I = \{t: 0 \leq t_j \leq 1, j = 1, \dots, N\}$. Let $I_0 = \{t: t_j = 0 \text{ for some } 1 \leq j \leq N\} \subset I$ be the “faces” of I which contain the origin $(0, \dots, 0)$. The IG characteristic is then defined as

$$\chi_{IG}(b) = \psi(A_b) - \psi(A_b \cap I_0).$$

The IG characteristic is the direct analogue of the number of “upcrossings” of a threshold b by a one-dimensional process $X(t)$. Adler (1981) shows that the IG characteristic is in fact invariant under a permutation of the coordinate axes, so that \mathcal{E}_u could be replaced by $\{t \in I: t_j = u\}$ for any $1 \leq j \leq N$. For more general sets that are the union of a finite number of intervals which only intersect on $(N - 1)$ -dimensional faces, the IG characteristic is defined as the sum of the IG characteristics on each interval.

2.4. Expectation of the DT characteristic. Using the point-set representation given in Section 2.1, Adler and Hasofer (1976) and Adler (1981) give the expectation of the DT characteristic for a stationary random field $X(t)$. This result requires some conditions on the regularity of the process $X(t)$. Adler (1981) gives some simpler conditions on the correlation function of $X(t)$ which ensure that these conditions are met; one such example is the Gaussian correlation function used for the applications in Section 6. These conditions

depend on the *moduli of continuity* of X_j and X_{jk} inside C , defined as

$$\omega_j(h) = \sup_{\|t-s\|<h} |X_j(\mathbf{t}) - X_j(\mathbf{s})|, \quad \omega_{jk}(h) = \sup_{\|t-s\|<h} |X_{jk}(\mathbf{t}) - X_{jk}(\mathbf{s})|,$$

where the supremum is taken over all $\mathbf{t}, \mathbf{s} \in C$, $j, k = 1, \dots, N$.

THEOREM 1 [Adler (1981), Theorem 5.2.1, page 105]. *Assume that for any $\varepsilon > 0$,*

$$P\left(\max_{j,k} \{\omega_j(h), \omega_{jk}(h)\} > \varepsilon\right) = o(h^N) \quad \text{as } h \downarrow 0,$$

the second-order partial derivatives of X have finite variances, the joint density of $X, X_1, \dots, X_N, \mathbf{D}_{N-1}$ is continuous in each of its variables and the conditional density of X, X_1, \dots, X_{N-1} given X_N and the second-order derivatives X_{jk} , $1 \leq j \leq N$, $1 \leq k \leq N-1$, is bounded above. Let $\phi_{N-1}(x, x_1, \dots, x_{N-1})$ be the density of X, X_1, \dots, X_{N-1} , so that $\phi_0(x)$ is the density of X , and define the rate of the DT characteristic as

$$\rho_N(b) = E\{X_N^+ \det(\mathbf{D}_{N-1}) | X = b, X_1 = 0, \dots, X_{N-1} = 0\} \phi_{N-1}(b, 0, \dots, 0).$$

Then the expected DT characteristic is

$$E\{\chi_{\text{DT}}(b)\} = |C| \rho_N(b),$$

where $|C|$ is the Lebesgue measure of C .

Adler [(1981), Theorem 5.3.1] shows that the rate of the DT characteristic for a Gaussian field has the following very simple form:

$$(2.3) \quad \rho_N(b) = \det(\Lambda)^{1/2} (2\pi)^{-(N+1)/2} \text{He}_{N-1}(b) \exp(-b^2/2),$$

where $\Lambda = \text{Var}[\partial X(\mathbf{t})/\partial \mathbf{t}]$ is the $N \times N$ variance matrix of the derivatives of the field and $\text{He}_{N-1}(b)$ is the Hermite polynomial of degree $N-1$ in b . Worsley (1994a) extends this result to χ^2 , t and F fields.

2.5. The choice of characteristic. The definitions of the characteristics appear superficially to be unrelated. However, Adler (1981) shows that within the domain of definition of all characteristics, and when the excursion set does not touch the boundary of $C = I$, then the characteristics are equal, and equal the Euler or Euler–Poincaré characteristic of the excursion set, that is, $\chi_{\text{DT}}(b) = \chi_{\text{HA}}(b) = \chi_{\text{IG}}(b)$. The proof of this relies on Morse's theorem, an important result from differential topology. In two and three dimensions the difference between the characteristics comes from points on the boundary of I .

From our point of view, an important advantage of the DT characteristic is that it has a point-set representation in all dimensions. It is this key feature which enabled Adler and Hasofer (1976) and Adler (1981) to find the expectation of the DT characteristic in all dimensions as given in Theorem 1. Point-set representations for the IG characteristic are more difficult to obtain. Adler (1981) gives such a representation for the IG characteristic in two

dimensions. It is easy to show using symmetry arguments that for stationary fields the expectation of the IG characteristic is the same as that of the DT characteristic, at least in two and three dimensions. Another advantage of the DT characteristic is that it is defined over arbitrary sets, such as the brain, whereas the IG characteristic is only defined over intervals.

However, from a practical point of view the IG characteristic has one overriding advantage: Adler [(1977) and (1981), page 117] gives a very simple method, based on Serra (1969), of approximating its value when $X(\mathbf{t})$ is sampled on a finite lattice of voxels. On the other hand, approximation of the DT characteristic would involve some very awkward calculations of the curvature of contours of $X(\mathbf{t})$. The fact that the IG characteristic is only defined over intervals or a finite union of intervals is still a disadvantage, but in practice the brain C is approximated by the union of a large number of intervals or “voxels.”

The last drawback is that both the DT and the IG characteristics are not invariant under rotations and reflections of the coordinate system, as illustrated in two dimensions in Figure 2, although this will occur rarely if the threshold is large. Worsley, Evans, Marrett and Neelin (1992) partially overcame this by using what we shall refer to as the AIG characteristic, $\chi_{\text{AIG}}(b)$, the average of $\chi_{\text{IG}}(b)$ over all reflections of the coordinate axes formed by replacing t_j by $1 - t_j$, $1 \leq j \leq N$. Note that $\chi_{\text{IG}}(b)$ is already invariant under permutations of the axes. Similar methods have been used by Gott, Melott and Dickinson (1986). This will obviously not affect its expectation, but it does mean that the AIG characteristic takes fractional values. These fractional values turn out to have a simple interpretation: if a connected component of the excursion set with no holes touches the boundary (see Figure 2), then its contribution to the AIG characteristic decreases below 1. Its value depends on the shape of the boundary where the excursion set touches. If the boundary is flat, then the contribution is $\frac{1}{2}$; if it is convex, then the contribution lies between 0 and $\frac{1}{2}$; if it is concave, then the contribution lies between $\frac{1}{2}$ and 1. Thus the AIG characteristic measures, in some sense, the proportion of the solid angle of a connected component of the excursion set that lies in C . This is close in spirit to Poincaré’s interpretation of the Euler characteristic as the integrated curvature of the boundary of A inside C .

In practice, regions of activation in PET images frequently occur in the cortex of the brain which is close to the boundary of C and so these regions are partially missed by the AIG characteristic. The Hadwiger characteristic seems to overcome all these difficulties. It takes integer values, it counts regions near the boundary, it is defined on any set C and it is invariant under any rotations or reflections.

3. The Hadwiger characteristic in two dimensions.

3.1. *Point-set representation.* A crucial step in deriving statistical properties of excursion characteristics is to obtain a point-set representation which

expresses the characteristic in terms of *local* properties of the excursion set rather than *global* properties such as connectedness. The definition of the DT characteristic is already a point-set representation. Adler [(1981), page 84] gives a point-set representation of the IG characteristic in $N = 2$ dimensions similar to that of the DT characteristic, provided realisations of the field $X(\mathbf{t})$ satisfy the same regularity conditions as those required for the DT characteristic. We shall now do the same for the Hadwiger characteristic.

We shall assume that ∂C , the boundary of C , is smooth except at a finite number of points. At a point $\mathbf{t} \in \partial C$, let X_{\perp} denote the derivative of $X(\mathbf{t})$ in the direction of t_1 pointing into C , so that $X_{\perp} = X_1$ if \mathbf{t} is on the left boundary of C and $X_{\perp} = -X_1$ if \mathbf{t} is on the right boundary of C (see Figure 3). For points where the tangent to ∂C is parallel to the t_1 axis, let $X_{\perp} = X_1$ when the tangent is above ∂C and let $X_{\perp} = -X_1$ when the tangent is below ∂C . Let X_U denote the derivative of X tangent to ∂C in the positive direction of t_2 . Finally, let ∂C_H be the set of points in ∂C that contribute to $\psi(C)$, the Hadwiger characteristic of C , and let $\psi(C; \mathbf{t})$ be their contribution at \mathbf{t} , so that

$$(3.1) \quad \psi(C) = \sum_{\partial C_H} \psi(C; \mathbf{t}),$$

where the summations are taken over \mathbf{t} (see Figure 3, points A and B).

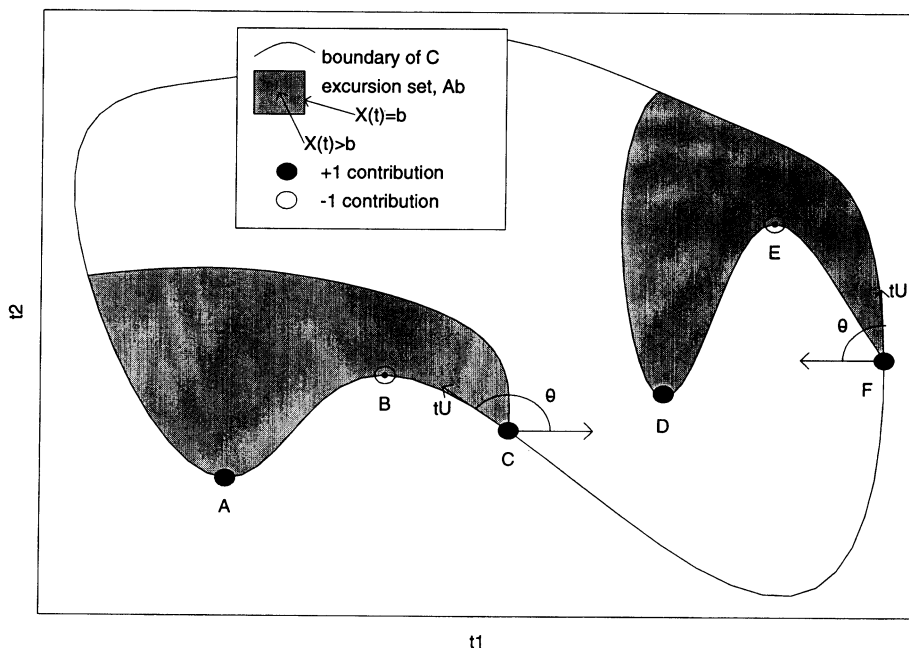


FIG. 3. Contributions to the Hadwiger characteristic in \mathbb{R}^2 .

LEMMA 1. Assume that the field $X(\mathbf{t})$, $\mathbf{t} \in \mathbb{R}^2$, satisfies the same regularity conditions given in Section 2.1. Let

$$\psi_B = \sum_{\partial C} (X = b)(X_{\perp} < 0)(X_U > 0) \quad \text{and} \quad \psi_H = \sum_{\partial C_H} (X \geq b)\psi(C; \mathbf{t}).$$

Then with probability 1,

$$\chi_{HA}(b) = \chi_{DT}(b) + \psi_B + \psi_H.$$

PROOF. We shall drop the subscript b and write $A = A_b$ throughout this proof. Recall that the definition of the Hadwiger characteristic is

$$\psi(A) = \sum_u \{ \psi(A \cap \mathcal{E}_u) - \psi(A \cap \mathcal{E}_{u-}) \},$$

where $\mathcal{E}_u = \{ \mathbf{t} \in C: t_2 = u \}$ and $\mathbf{t} = (t_1, t_2) \in \mathbb{R}^2$. We shall start with the case where ∂C is smooth. For points in the interior of C , Adler [(1981), Section 4.2], shows that their contribution to the IG characteristic, and hence the Hadwiger characteristic, is the same as the DT characteristic of A in C : points with $X = b$, $X_{\perp} = 0$ and $X_2 > 0$ contribute $+1$ if $X_{11} < 0$ and -1 if $X_{11} > 0$, respectively, to $\psi(A)$ (Figure 3, points D and E , respectively). We now consider the boundary ∂C . If $X = b$, $X_{\perp} < 0$ and $X_U > 0$, then $\psi(A \cap \mathcal{E}_u) = 1$, $\psi(A \cap \mathcal{E}_{u-}) = 0$ and this point contributes $+1$ to $\psi(A)$ (Figure 3, points C and F). Finally, points in ∂C_H that contribute to $\psi(C)$ will also contribute to $\psi(A)$ whenever $X \geq b$ (Figure 3, points A and B). Summing over all these regions gives the result for a smooth boundary. It is now straightforward to extend the result to the case where there are a finite number of points where ∂C is not smooth, since if these points lie in $\partial C \setminus \partial C_H$, then they will almost surely never contribute to $\psi(A)$. \square

3.2. *Expectation.* We shall use the notation $d\mathbf{u}$, where \mathbf{u} is a unit vector, to denote the unsigned scalar differential in the direction of \mathbf{u} .

LEMMA 2. Assume that the conditions of Theorem 1 hold. Let \mathbf{t}_U denote a unit vector tangent to ∂C in the positive direction of t_2 . Then

$$E(\psi_B) = \int_{\partial C} E\{(X_{\perp} < 0)X_U^+ | X = b\} \phi_0(b) d\mathbf{t}_U.$$

PROOF. We evaluate the expectation of the point-set representations given in Lemma 1 following the methods used to prove Theorem 5.1.1 of Adler [(1981), page 95]. For any $\varepsilon > 0$ let $\delta_{\varepsilon}(x)$ be a function of \mathbb{R} defined to be $1/(2\varepsilon)$ on $|x| < \varepsilon$ and 0, elsewhere. Under the conditions of the above theorem applied to the point-set representation of ψ_B we have

$$\psi_B = \lim_{\varepsilon \rightarrow 0} \int_{\partial C} \delta_{\varepsilon}(X - b)(X_{\perp} < 0)(X_U > 0) J d\mathbf{t}_U,$$

where J is the Jacobian

$$J = \left| \frac{\partial(X - b)}{\partial \mathbf{t}_U} \right| = |X_U|.$$

Following a similar method of proof to that of Theorem 5.2.1 of Adler [(1981), page 105], we obtain the result. \square

3.3. Isotropic fields.

THEOREM 2. *Assume that the conditions of Theorem 1 hold for an isotropic stationary random field $X(\mathbf{t})$, $\mathbf{t} \in \mathbb{R}^2$. Then*

$$E\{\chi_{\text{HA}}(b)\} = |C| \rho_2(b) + |\partial C| \rho_1(b)/2 + \psi(C)P(X \geq b).$$

where $|\partial C|$ is the perimeter length of C .

PROOF. We take expectations term by term of the result of Lemma 1. The first term follows from Theorem 1. For the second term, we evaluate the expectations in Lemma 2 by changing to polar coordinates. Let $X_{\perp} = r \cos \alpha$ and $X_2 = r \sin \alpha$, $r \geq 0$, $0 \leq \alpha < 2\pi$. Let θ be the angle between \mathbf{t}_U and the direction of \mathbf{t}_1 pointing inside C , $0 \leq \theta < \pi$, so that

$$X_U = X_{\perp} \cos \theta + X_2 \sin \theta = r \cos(\alpha - \theta);$$

see Figure 3. Since the field is isotropic, then α is uniformly distributed on $[0, 2\pi)$ independent of r , conditional on X . Thus

$$\begin{aligned} E\{(X_{\perp} < 0)X_U^+ | X\} &= E\{(\cos \alpha < 0)r \cos(\alpha - \theta)[\cos(\alpha - \theta) > 0] | X\} \\ &= E\{(\pi/2 < \alpha < \pi/2 + \theta)r \cos(\alpha - \theta) | X\} \\ &= E(r | X) \int_{\pi/2}^{\pi/2 + \theta} \cos(\alpha - \theta) d\theta / (2\pi) \\ &= E(r | X)(1 - \cos \theta) / (2\pi). \end{aligned}$$

Integrating around the boundary of C we have

$$\int_{\partial C} (1 - \cos \theta) d\mathbf{t}_U = |\partial C|.$$

Converting back from polar coordinates,

$$\begin{aligned} (3.2) \quad E(r | X = b) &= \pi E\{(-\pi/2 < \alpha < \pi/2)r \cos \alpha / (2\pi) | X = b\} \\ &= \pi E(X_1^+ | X = b). \end{aligned}$$

Combining these results, we get

$$E(\psi_B) = \int_{\partial C} (1 - \cos \theta) d\mathbf{t}_U E(r | X = b) \phi_0(b) / (2\pi) = |\partial C| \rho_1(b) / 2.$$

The third term follows on taking expectations of ψ_H from Lemma 1 and (3.1). \square

4. Hadwiger characteristic in three dimensions.

4.1. Point-set representation. As for two dimensions in the previous section, we start with a point-set representation for the Hadwiger characteristic, find its expectation, then simplify it for the special case of an isotropic field.

We shall assume that ∂C is smooth except for a set ∂C_E of smooth edges or creases of finite length, where the tangent to ∂C exists in only one direction; and a finite set ∂C_V of vertices or corners, where no tangent exists in any direction.

We shall drop the subscript b and write $A = A_b$ throughout this section. Recall that the definition of the Hadwiger characteristic is

$$\psi(A) = \sum_u \{\psi(A \cap \mathcal{E}_u) - \psi(A \cap \mathcal{E}_{u-})\},$$

where $\mathcal{E}_u = \{\mathbf{t} \in C : t_3 = u\}$ and $\mathbf{t} = (t_1, t_2, t_3) \in \mathbb{R}^3$. For points in the interior of C , Adler [(1981), Section 4.2] shows that their contribution to the IG characteristic, and hence the Hadwiger characteristic, is the same as the DT characteristic of A in C : points with $X = b$, $X_1 = 0$, $X_2 = 0$ and $X_2 > 0$ contribute $+1$ if $\det(\mathbf{D}_2) > 0$ and -1 if $\det(\mathbf{D}_2) < 0$, respectively, to $\psi(A)$.

Let $\partial C_S = \partial C \setminus \partial C_E \setminus \partial C_V$ be the smooth portion of ∂C . There are two ways in which $\psi(A \cap \mathcal{E}_u)$ can differ from $\psi(A \cap \mathcal{E}_{u-})$. The first is when a point which contributes $+1$ to $\psi(A \cap \mathcal{E}_u)$ does not contribute to $\psi(A \cap \mathcal{E}_{u-})$ (Figure 4, point A). This will occur if $A \in \mathcal{E}_u$ contains only the point $\mathbf{t} = (t_1, t_2, u)$ and $A \cap \mathcal{E}_v$, $v < u$, is empty in a neighbourhood of \mathbf{t} . Let X_\perp denote the derivative of X in the plane \mathcal{E}_u in the direction of the inward normal to $\partial C \cap \mathcal{E}_u$. Let X_U denote the derivative of X tangent to ∂C , orthogonal to the plane \mathcal{E}_u in the positive (upward) direction of t_3 . Let X_T denote the derivative of X in the plane \mathcal{E}_u tangent to $\partial C \cap \mathcal{E}_u$, and let X_{TT}

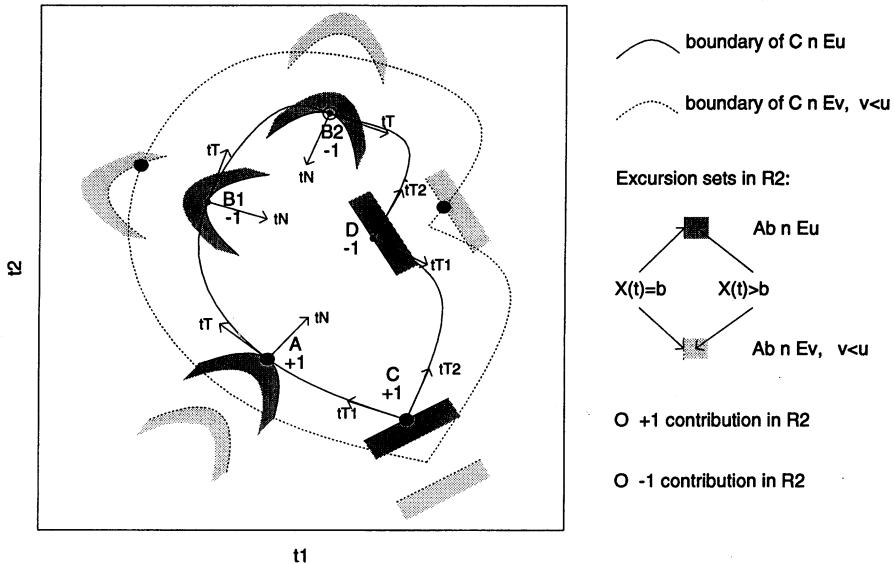


FIG. 4. Contributions to the Hadwiger characteristic in \mathbb{R}^3 . Two planes through C are shown schematically: $C \cap \mathcal{E}_u$, whose boundary is the inside curve, and $C \cap \mathcal{E}_v$, $v < u$, whose boundary is the outside curve. Portions of the excursion set in these planes are shown as shaded regions.

denote the second derivative of X in this direction. Finally, let c_{TT} denote the curvature of $\partial C \cap \mathcal{E}_u$ in the plane \mathcal{E}_u . By the implicit function theorem, the curvature of $\partial A \cap \mathcal{E}_u$ is $X_{TT}/(-X_\perp)$. Then $\partial A \cap \mathcal{E}_u$ will intersect $\partial C \cap \mathcal{E}_u$ only at the point \mathbf{t} in a neighbourhood of \mathbf{t} if $X_\perp < 0$, $X_T = 0$ and the curvature $X_{TT}/(-X_\perp)$ is less than c_{TT} . If in addition we have $X_U > 0$, then $\partial A \cap \mathcal{E}_u$ will not intersect $\partial C \cap \mathcal{E}_v$ in a neighbourhood of \mathbf{t} . We thus conclude that the point \mathbf{t} will contribute $+1$ to $\psi(A)$ if $X = b$ at \mathbf{t} , $X_\perp < 0$, $X_U > 0$, $X_T = 0$ and $X_{TT} + c_{TT}X_\perp < 0$.

The second possibility is that a point $\mathbf{t} = (t_1, t_2, u)$ does not contribute to $\psi(A \cap \mathcal{E}_u)$ but contributes $+1$ to $\psi(A \cap \mathcal{E}_{u-})$ (Figure 4, point $B1$), or \mathbf{t} contributes -1 to $\psi(A \cap \mathcal{E}_u)$ but does not contribute to $\psi(A \cap \mathcal{E}_{u-})$ (Figure 4, point $B2$), making a contribution of -1 to $\psi(A)$ in either case. This will occur when $\partial C \cap \mathcal{E}_u$ contains $\partial A \cap \partial C \cap \mathcal{E}_u$ in a neighbourhood of \mathbf{t} , but $\partial A \cap \partial C \cap \mathcal{E}_v$, $v < u$, contains a ‘‘hole.’’ Following the same reasoning as above, this will happen when $X = b$ at \mathbf{t} , $X_\perp < 0$, $X_U > 0$, $X_T = 0$ and the curvature of $\partial A \cap \mathcal{E}_u$ is greater than the curvature of $\partial C \cap \mathcal{E}_u$, that is, if $X_{TT} + c_{TT}X_\perp > 0$. Combining these two types of contribution, we obtain, on summing over \mathbf{t} ,

$$\begin{aligned} \psi_S = \sum_{\partial C_S} (X = b)(X_\perp < 0)(X_U > 0)(X_T = 0) \\ \times \{ (X_{TT} + c_{TT}X_\perp < 0) - (X_{TT} + c_{TT}X_\perp > 0) \}. \end{aligned}$$

We now consider points $\mathbf{t} = (t_1, t_2, u)$ at the intersection of an edge ∂C_E and the plane \mathcal{E}_u . We shall partition ∂C_E into two sets: those points where $\partial C \cap \mathcal{E}_u$ is convex, denoted by ∂C_{E+} (Figure 4, point C), and those points where $\partial C \cap \mathcal{E}_u$ is concave, denoted by ∂C_{E-} (Figure 4, point D). We shall first assume that $\partial C \cap \mathcal{E}_u$ is convex at \mathbf{t} . Then \mathbf{t} will contribute $+1$ to $\psi(A)$ if $A \cap \mathcal{E}_u$ contains only the point \mathbf{t} and $A \cap \mathcal{E}_v$, $v < u$, is empty in a neighbourhood of \mathbf{t} . Let X_E denote the derivative of X tangent to the edge ∂C_E in the positive (upward) direction of t_3 . Let X_{T1} and X_{T2} denote the two derivatives of X in the plane \mathcal{E}_u in the direction of the two tangents to $\partial C \cap \mathcal{E}_u$ on either side of the edge at \mathbf{t} . Then \mathbf{t} will contribute $+1$ to $\psi(A)$ if $X = b$ at \mathbf{t} , $X_E > 0$, $X_{T1} < 0$ and $X_{T2} < 0$. Next we shall assume that $\partial C \cap \mathcal{E}_u$ is concave at \mathbf{t} . Then \mathbf{t} will contribute -1 to $\psi(A)$ if $\partial C \cap \mathcal{E}_u$ contains $\partial A \cap \partial C \cap \mathcal{E}_u$ in a neighbourhood of \mathbf{t} , but $\partial A \cap \partial C \cap \mathcal{E}_v$, $v < u$, contains a ‘‘hole.’’ This will occur if $X = b$ at \mathbf{t} , $X_E > 0$, $X_{T1} > 0$ and $X_{T2} > 0$. Combining these two types of contribution, we obtain, on summing over \mathbf{t} ,

$$\begin{aligned} \psi_E = \sum_{\partial C_{E+}} (X = b)(X_E > 0)(X_{T1} < 0)(X_{T2} < 0) \\ - \sum_{\partial C_{E-}} (X = b)(X_E > 0)(X_{T1} > 0)(X_{T2} > 0). \end{aligned}$$

Finally let ∂C_H be the set of points in ∂C that contribute to $\psi(C)$ and let

$\psi(C; \mathbf{t})$ be their contribution at \mathbf{t} , so that on summing over \mathbf{t} ,

$$\psi(C) = \sum_{\partial C_H} \psi(C; \mathbf{t})$$

as in two dimensions. These points will also contribute to $\psi(A)$ whenever $X \geq b$, so that their contribution to $\psi(A)$ is

$$(4.1) \quad \psi_H = \sum_{\partial C_H} (X \geq b) \psi(C; \mathbf{t}).$$

Vertices in ∂C_V not included in any of the above contributions will almost surely never contribute to $\psi(A)$. We have thus proved the following result.

LEMMA 3. Assume that the field $X(\mathbf{t})$, $\mathbf{t} \in \mathbb{R}^3$, satisfies the same regularity conditions given in Section 2.1. Then with probability 1,

$$\chi_{HA}(b) = \chi_{DT}(b) + \psi_S + \psi_E + \psi_H.$$

4.2. *Expectation.* The next result gives the expectation of contributions to $\psi(A)$ from the smooth part of ∂C .

LEMMA 4. Assume that the conditions of Theorem 1 hold. Let \mathbf{t}_T be a unit vector in the plane \mathcal{E}_u tangent to $\partial C \cap \mathcal{E}_u$ and let \mathbf{t}_U be a unit vector orthogonal to \mathbf{t}_T and tangent to ∂C , pointing in the positive (upward) direction of t_3 at the point $\mathbf{t} = (t_1, t_2, u)$. Let $\phi_T(x, x_T)$ be the density of (X, X_T) . Then

$$E(\psi_S) = - \iint_{\partial C_S} E\{(X_{\perp} < 0) X_U^+(X_{TT} + c_{TT} X_{\perp}) \mid X = b, X_T = 0\} \\ \times \phi_T(b, 0) d\mathbf{t}_T d\mathbf{t}_U.$$

PROOF. We evaluate the expectation of the point-set representations given in Lemma 3 following the methods used to prove Theorem 5.1.1 of Adler [(1981), page 95]. For any $\varepsilon > 0$ let $b(\varepsilon)$ be the ball of radius ε defined by $b(\varepsilon) = \{(x_1, x_2) : \|(x_1, x_2)\| < \varepsilon\}$ and $\delta_{\varepsilon}(x_1, x_2)$ is a function on \mathbb{R}^2 defined to be constant on $b(\varepsilon)$ and zero elsewhere, normalised so that $\int \delta_{\varepsilon}(x_1, x_2) dx_1 dx_2 = 1$. Under the conditions of the above Theorem applied to the point-set representation of ψ_S we have

$$\psi_S = \lim_{\varepsilon \rightarrow 0} \iint_{\partial C_S} \delta_{\varepsilon}(X - b, X_T) (X_{\perp} < 0) (X_U > 0) \\ \times \{(X_{TT} + c_{TT} X_{\perp} < 0) - (X_{TT} + c_{TT} X_{\perp} > 0)\} J d\mathbf{t}_T d\mathbf{t}_U,$$

where J is the Jacobian

$$J = \left| \det \left(\frac{\partial (X - b, X_T)}{\partial (\mathbf{t}_T, \mathbf{t}_U)} \right) \right| = |X_T X_{TU} - X_U (X_{TT} + c_{TT} X_{\perp})|$$

and X_{TU} is the partial derivative of X with respect to \mathbf{t}_T and \mathbf{t}_U . Note that

as $\varepsilon \rightarrow 0$, $X_T \rightarrow 0$ and so

$$\begin{aligned} & (X_U > 0) \{ (X_{TT} + c_{TT} X_\perp < 0) - (X_{TT} + c_{TT} X_\perp > 0) \} J \\ & \rightarrow -X_U^+ (X_{LTT} + c_{TT} X_\perp). \end{aligned}$$

Following a similar method of proof to that of Theorem 5.2.1 of Adler [(1981), page 105], we obtain the result. \square

The next result gives the expectation of contributions to $\psi(A)$ from edges of ∂C . The proof is similar to that of Lemma 2 and is omitted.

LEMMA 5. *Assume that the conditions of Theorem 1 hold. Let \mathbf{t}_E denote the unit vector tangent to the edge ∂C_E in the positive (upward) direction of t_3 . Then*

$$\begin{aligned} E(\psi_E) &= \int_{\partial C_{E^+}} E\{(X_{T1} < 0)(X_{T2} < 0)X_E^+ \mid X = b\} \phi_0(b) \, d\mathbf{t}_E \\ &\quad - \int_{\partial C_{E^-}} E\{(X_{T1} > 0)(X_{T2} > 0)X_E^+ \mid X = b\} \phi_0(b) \, d\mathbf{t}_E. \end{aligned}$$

4.3. *Isotropic fields.* The next two lemmas give simplified expressions for the expectations in Lemmas 4 and 5 for isotropic fields. The proofs are tedious and have been relegated to the Appendix.

LEMMA 6. *Assume that the conditions of Theorem 1 hold for an isotropic stationary random field $X(\mathbf{t})$, $\mathbf{t} \in \mathbb{R}^3$. Let θ be the angle between the outward normal to ∂C and the positive direction of the t_3 axis, $0 \leq \theta < \pi$. Then*

$$E(\psi_S) = |\partial C| \rho_2(b)/2 + \iint_{\partial C_S} c_{TT} (\sin \theta - \theta \cos \theta) \, d\mathbf{t}_T \, d\mathbf{t}_U \, \rho_1(b)/(2\pi),$$

where $|\partial C|$ is the surface area of C .

LEMMA 7. *Assume that the conditions of Theorem 1 hold for an isotropic stationary random field $X(\mathbf{t})$, $\mathbf{t} \in \mathbb{R}^3$. Let θ_1 and θ_2 be the angles between the positive direction of the t_3 axis and the two outward normals to ∂C on either side of an edge in ∂C_E in a neighbourhood of \mathbf{t} , $0 \leq \theta_1 < \pi$, $0 \leq \theta_2 < \pi$. Let ω_1 and ω_2 be the angles between the tangent to the edge in the positive (upward) direction of t_3 at $\mathbf{t} = (t_1, t_2, u)$ and the two tangents to $\partial C \cap \mathcal{E}_u$ in \mathcal{E}_u on either side of the edge at \mathbf{t} . Finally, let δ be the internal angle of ∂C at \mathbf{t} between the two tangent planes to ∂C on either side of the edge. Then*

$$E(\psi_E) = \int_{\partial C_E} (\pi - \delta - \theta_1 \cos \omega_1 - \theta_2 \cos \omega_2) \, d\mathbf{t}_E \, \rho_1(b)/(2\pi).$$

We now have all the ingredients for the expectation of the Hadwiger characteristic in three dimensions, but before putting them together, we shall

prove the following lemma, which we shall use to put the result in a more familiar form. The proof is once again relegated to the Appendix. Let c_{\max} and c_{\min} be the maximum and minimum inside curvatures, respectively, of ∂C_S at a point \mathbf{t} in planes normal to the tangent plane at \mathbf{t} ; c_{\max} and c_{\min} are also known as the principal curvatures of ∂C_S .

LEMMA 8. *Let S be a subset of ∂C_S with a boundary ∂S that is composed of a finite number of piecewise smooth curves. Let $\theta, \mathbf{t}_U, \mathbf{t}_T, c_{TT}, c_{\max}$ and c_{\min} be defined as above. Let \mathbf{r} denote a unit vector tangent to ∂S , pointing in the same direction around ∂S , and let ω be the angle between \mathbf{r} and \mathbf{t}_T . Then*

$$\iint_S c_{TT}(\sin \theta - \theta \cos \theta) d\mathbf{t}_T d\mathbf{t}_U - \int_{\partial S} \theta \cos \omega d\mathbf{r} = \iint_S (c_{\max} + c_{\min}) d\mathbf{t}_T d\mathbf{t}_U.$$

We now come to our main theorem. Define

$$H(\partial C) = \left(\iint_{\partial C_S} (c_{\max} + c_{\min}) d\mathbf{t}_T d\mathbf{t}_U + \int_{\partial C_E} (\pi - \delta) d\mathbf{t}_E \right) / 2.$$

If ∂C is smooth everywhere, so that the second term is zero, then $H(\partial C)$ is known as the mean curvature of ∂C [see Santaló (1976), page 222]. If C is a polyhedron, so that the first term is zero, then $H(\partial C)$ is half the sum of the lengths of the edges of C multiplied by their angular deficiency. If C is convex, let $\Delta(C)$ be the average, over all rotations, of the maximum perpendicular distance between two parallel planes that touch ∂C ; this is known in stereology as the mean caliper diameter of C . Then it can be shown that $\Delta(C) = H(\partial C)/(2\pi)$ [see Santaló (1976), page 226]. Values of $H(\partial C)$ for some common geometric solids are given by Santaló [(1976), page 229].

THEOREM 3. *Assume that the conditions of Theorem 1 hold for an isotropic stationary random field $X(\mathbf{t}), \mathbf{t} \in \mathbb{R}^3$. Then*

$$E\{\chi_{\text{HA}}(b)\} = |C| \rho_3(b) + |\partial C| \rho_2(b)/2 + H(\partial C) \rho_1(b)/\pi + \psi(C)P(X \geq b).$$

PROOF. Combining Lemmas 3, 6, 7 and result (4.1) we get

$$E\{\chi_{\text{HA}}(b)\} = |C| \rho_3(b) + |\partial C| \rho_2(b)/2 + L \rho_1(b)/(2\pi) + \psi(C)P(X \geq b),$$

where

$$L = \iint_{\partial C_S} c_{TT}(\sin \theta - \theta \cos \theta) d\mathbf{t}_U d\mathbf{t}_T - \int_{\partial C_E} \theta_1 \cos \omega_1 d\mathbf{t}_E - \int_{\partial C_E} \theta_2 \cos \omega_2 d\mathbf{t}_E + \int_{\partial C_E} (\pi - \delta) d\mathbf{t}_E.$$

Let us partition the surface of C into a finite number of components, each with a piecewise smooth boundary. This can be done, for example, by incorporating the edges ∂C_E and the vertices ∂C_V into the boundaries of the components of the partition. Then Lemma 8 can be applied to each compo-

nent and summed over all components. Clearly the surface integrals add to give the surface integral of $2H(\partial C)$. Consider the boundary where two adjacent components of the partition meet. The line integrals around the boundary of one partition will contribute $-\int \theta_1 \cos \omega_1 d\mathbf{t}_E$ and the line integral around the boundary of the second will contribute $-\int \theta_2 \cos \omega_2 d\mathbf{t}_E$. This contribution is zero if the components do not meet on an edge of C , since $\theta_1 = \theta_2$ and $\omega_1 + \omega_2 = \pi$. The summation of Lemma 8 applied to all components thus equals the first three integrals of L and so $L = 2H(\partial C)$. \square

Applying Theorem 3 to a sphere C of radius a , we have $|C| = (4/3)\pi a^3$, $|\partial C| = 4\pi a^2$, $c_{\max} = c_{\min} = 1/a$, $H(\partial C) = 4\pi a$, ∂C_E is empty, $\psi(C) = 1$ and so

$$E\{\chi_{\text{HA}}(b)\} = (4/3)\pi a^3 \rho_3(b) + 2\pi a^2 \rho_2(b) + 4a \rho_1(b) + P(X \geq b).$$

For C a cube of side h , we have $|C| = h^3$, $|\partial C| = 6h^2$, $c_{\max} = c_{\min} = 0$, $\pi - \delta = \pi/2$, $H(\partial C) = 3\pi h$, $\psi(C) = 1$ and so

$$(4.2) \quad E\{\chi_{\text{HA}}(b)\} = h^3 \rho_1(b) + 3h^2 \rho_2(b) + 3h \rho_1(b) + P(X \geq b).$$

4.4. *Application to surfaces embedded in \mathbb{R}^3 .* We can use the result of Theorem 3 to find the expected Hadwiger characteristic of the intersection of the excursion set of an isotropic stationary field in \mathbb{R}^3 with a piecewise smooth surface S . Suppose we form a solid S_h by “thickening” S by a small amount h . If we apply Theorem 3 to S_h and let the thickness h tend to zero, then the first term vanishes since the volume of S_h tends to zero. The second term approaches $|S| \rho_2(b)$. As h approaches zero, the curvatures and angular deficiencies cancel on either side of S_h , the mean curvature $H(\partial S_h)$ approaches $|\partial S|/\pi/2$, and so the third term approaches $|\partial S| \rho_1(b)/2$. Since $\psi(S_h)$ approaches $\psi(S)$, the last term is just $\psi(S)P(X \geq b)$ and so we have

$$(4.3) \quad E\{\chi_{\text{HA}}(b)\} = |S| \rho_2(b) + |\partial S| \rho_1(b)/2 + \psi(S)P(X \geq b).$$

It is rather surprising that this is identical to the result of Theorem 2 in two dimensions, obviously a special case of (4.3) when S is flat. Thus no matter how S is folded or even creased, the expectation of the Hadwiger characteristic is given by (4.3). If S is homeomorphic to the surface of a sphere, so that it has no boundary, then $E\{\chi_{\text{HA}}(b)\} = |S| \rho_2(b) + 2P(X \geq b)$ since the surface of a sphere has a Hadwiger characteristic of 2. This result has been given by Gott, Park, Juszkievicz, Bies, Bennett, Bouchet and Stebbins (1990), where it is applied to the cosmic microwave background, which is modelled as a random field on the surface of a sphere.

5. Alternative derivations for isotropic fields. In the next two subsections we shall use a heuristic argument, based on the kinematic fundamental formula of integral geometry [see Santaló (1976), page 113], to find the expected Euler–Poincaré characteristic of the excursion set of an isotropic random field. Because the Euler–Poincaré characteristic equals the Hadwiger

characteristic within the domain of definition of both, we shall see that results for the Euler–Poincaré characteristic agree with those for the Hadwiger characteristic given by Theorems 2 and 3.

5.1. *Kinematic fundamental formula in two dimensions.* Let B and C be two sets in \mathbb{R}^2 bounded by a finite number of piecewise smooth curves. Suppose B is fixed and C moves rigidly under rotations and translations, and assume that for all positions of C the intersection $B \cap C$ has a finite number of connected components. Let $\chi(A)$ be the Euler–Poincaré characteristic of a set A . Then the kinematic fundamental formula states that

$$(5.1) \quad \int \chi(B \cap C) = 2\pi\{|B|\chi(C) + |C|\chi(B)\} + |\partial B||\partial C|,$$

where the integral is over all rotations and translations of C [see Santaló (1976), page 113]. Let S be a fixed disk of large radius s and suppose C moves relative to S . As s tends to infinity, the proportion of positions of C in which C intersects the boundary of S , relative to the interior of S , will tend to zero. Applying the kinematic fundamental formula to S and C we obtain $\int \chi(S \cap C)/|S| \rightarrow 2\pi$ as $s \rightarrow \infty$, over all movements of C . Now let B be the excursion set of an isotropic random field $X(\mathbf{t})$ inside S above the threshold b , $B = \{\mathbf{t} \in S: X(\mathbf{t}) \geq b\}$. If $X(\mathbf{t})$ satisfies the conditions of Theorem 1, then B is almost surely bounded by a finite number of piecewise smooth curves. Now suppose that $X(\mathbf{t})$ is fixed so that B is fixed, but C moves relative to B . Applying the kinematic fundamental formula to B and C , normalising by $2\pi|S|$ and writing $A = B \cap C$ for the excursion set of $X(\mathbf{t})$ inside C , we have

$$\frac{\int \chi(A)}{2\pi|S|} = \frac{|B|}{|S|}\chi(C) + |C|E\left(\frac{\chi(B)}{|S|}\right) + E\left(\frac{|\partial B|}{|S|}\right)\frac{|\partial C|}{2\pi}.$$

Taking expectations over $X(\mathbf{t})$, letting s tend to infinity and noting that $X(\mathbf{t})$ is isotropic, the right-hand side converges to $E\{\chi(A)\}$ and we obtain

$$E\{\chi(A)\} = \lim_{s \rightarrow \infty} \left\{ E\left(\frac{|B|}{|S|}\right)\chi(C) + |C|E\left(\frac{\chi(B)}{|S|}\right) + E\left(\frac{|\partial B|}{|S|}\right)\frac{|\partial C|}{2\pi} \right\}.$$

Now $E(|B|/|S|) \rightarrow P(X \geq b)$ and $E\{\chi(B)/|S|\} \rightarrow \rho_2(b)$ as $s \rightarrow \infty$. The last term is proportional to the mean boundary length of the excursion set per unit area, which can be found by another application of the kinematic fundamental formula to the special case where C is a thin rectangle T of length l and breadth h . We then have

$$E\{\chi(B \cap T)\} = P(X \geq b) + lh\rho_2(b) + \lim_{s \rightarrow \infty} E\left(\frac{|\partial B|}{|S|}\right)\frac{2(l+h)}{2\pi}.$$

Dividing both sides by l and letting $l \rightarrow \infty$ and $h \rightarrow 0$, so that T approaches a line, the left-hand side approaches the rate $\rho_1(b)$ of the Euler characteristic of the excursion set along a line, and we have $\lim_{s \rightarrow \infty} E(|\partial B|/|S|) = \pi\rho_1(b)$.

Combining these results we obtain

$$(5.2) \quad E\{\chi(A)\} = |C|\rho_2(b) + |\partial C|\rho_1(b)/2 + \chi(C)P(X \geq b),$$

which is identical to the result of Theorem 2.

5.2. *Kinematic fundamental formula in three dimensions.* Let B and C be two sets in \mathbb{R}^3 bounded by smooth surfaces except for a finite number of smooth edges of finite length and a finite number of vertices. Suppose B is fixed and C moves rigidly under rotations and translations, and assume that for all positions of C the intersection $B \cap C$ has a finite number of connected components. Then the kinematic fundamental formula states that

$$(5.3) \quad \int \chi(B \cap C) = 8\pi^2\{|B|\chi(C) + |C|\chi(B)\} \\ + 2\pi\{|\partial B|H(\partial C) + |\partial C|H(\partial B)\},$$

where the integral is over all rotations and translations of C [see Santaló (1976), page 262]. Let S be a fixed ball of large radius s and suppose C moves relative to S . Applying the kinematic fundamental formula to S and C we obtain $\int \chi(S \cap C)/|S| \rightarrow 8\pi^2$, as $s \rightarrow \infty$. Now let $B = \{\mathbf{t} \in S: X(\mathbf{t}) \geq b\}$, where $X(\mathbf{t})$ is an isotropic random field satisfying the conditions of Theorem 1. Applying the kinematic fundamental formula to B and C , normalising by $8\pi^2|S|$ and writing $A = B \cap C$ for the excursion set of $X(\mathbf{t})$ inside C , we have

$$\frac{\int \chi(A)}{8\pi^2|S|} = \frac{|B|}{|S|}\chi(C) + |C|\frac{\chi(B)}{|S|} + \left\{ \frac{|\partial B|}{|S|}H(\partial C) + |\partial C|\frac{H(\partial B)}{|S|} \right\} / 4\pi.$$

Taking expectations over $X(\mathbf{t})$, letting s tend to infinity and noting that $X(\mathbf{t})$ is isotropic, we obtain

$$E\{\chi(A)\} = \lim_{s \rightarrow \infty} \left\{ E\left(\frac{|B|}{|S|} \right) \chi(C) + |C| E\left(\frac{\partial(B)}{|S|} \right) \right\} \\ + \lim_{s \rightarrow \infty} \left\{ E\left(\frac{|\partial B|}{|S|} \right) H(\partial C) + |\partial C| E\left(\frac{H(\partial B)}{|S|} \right) \right\} / 4\pi.$$

As before, $E(|B|/|S|) \rightarrow P(X \geq b)$ and $E\{\chi(B)/|S|\} \rightarrow \rho_3(b)$ as $s \rightarrow \infty$. The third term is proportional to the mean surface area of the excursion set per unit volume, which can be found by another application of the kinematic fundamental formula to the special case where C is a cylinder T of radius l and height h . We then have $H(\partial T) = \pi h + \pi^2 l$ [Santaló (1976), page 230] and so

$$(5.4) \quad E\{\chi(B \cap T)\} = P(X \geq b) + \pi l^2 h \rho_3(b) \\ + \lim_{s \rightarrow \infty} \left\{ E\left(\frac{|\partial B|}{|S|} \right) (\pi h + \pi^2 l) \right. \\ \left. + (2\pi l^2 + 2\pi lh) E\left(\frac{H(\partial B)}{|S|} \right) \right\} / 4\pi.$$

Dividing both sides of (5.4) by the height h and letting $l \rightarrow 0$ and $h \rightarrow \infty$, so that T approaches a line, the left-hand side approaches the rate $\rho_1(b)$ of the Euler characteristic of the excursion set on a line, and so $\lim_{s \rightarrow \infty} E\{|\partial B|/|S|\} = 2\pi\rho_1(b)$. Now dividing both sides of (5.4) by the base area πl^2 and letting $l \rightarrow \infty$ and $h \rightarrow 0$, so that T approaches a plane, the left-hand side approaches the rate $\rho_2(b)$ of the Euler characteristic of the excursion set in a plane, and so $\lim_{s \rightarrow \infty} E\{H(\partial B)/|S|\} = 4\rho_2(b)$. Combining these results we obtain

$$(5.5) \quad E\{\chi(A)\} = |C|\rho_3(b) + |\partial C|\rho_2(b)/2 + H(\partial C)\rho_1(b)/\pi\chi(C)P(X \geq b),$$

which is identical to the result of Theorem 3. This immediately suggests a generalisation to higher dimensions, but we shall not pursue it in this paper.

The similarity between (5.2) and Theorem 2 and between (5.5) and Theorem 3 runs deeper. A closer inspection of the proof of the kinematic fundamental formula, given for example by Santaló [(1976), pages 114 and 262], shows exactly how the terms in (5.1) and (5.3) arise. The proof uses the Gauss–Bonnet theorem which expresses the Euler–Poincaré characteristic of a set bounded by a piecewise smooth boundary as the product of the principal curvatures averaged over the boundary. The first term $|B|\chi(C)$ comes from the part of ∂C inside B ; this becomes the last term $\chi(C)P(X \geq b)$ of (5.2) and (5.5), which corresponds to the contribution of ∂C inside the excursion set in Theorems 2 and 3. The second term $|C|\chi(B)$ comes from the part of ∂B inside C ; this becomes the first term $|C|\rho_3(b)$ of (5.2) and (5.5), which corresponds to the contribution from the excursion set in the interior of C in Theorems 2 and 3. Finally the third and fourth terms of (5.1) and (5.3) come from the intersection of ∂B with ∂C which correspond with the contributions of Lemmas 2, 4 and 5.

5.3. *Small convex sets.* We can check the results of Theorems 2 and 3 for small compact convex sets $C \subset \mathbb{R}^N$ as follows. Let \mathbf{t} be an interior point of C and approximate $X(\mathbf{s})$, $\mathbf{s} \in C$, by the linear function

$$\tilde{X}(\mathbf{s}) = X + (\mathbf{s} - \mathbf{t})'\dot{\mathbf{X}},$$

where $\dot{\mathbf{X}} = \partial\mathbf{X}/\partial\mathbf{t} = (X_1, \dots, X_N)'$. Then $\chi_{\text{HA}}(b)$ is approximated by the Hadwiger characteristic of the excursion set of $\tilde{X}(\mathbf{s})$, which is 1 if its maximum, which must occur on ∂C , exceeds b and 0, otherwise. Thus

$$E\{\chi_{\text{HA}}(b)\} \approx P\left\{\max_{\mathbf{s} \in \partial C} \tilde{X}(\mathbf{s}) \geq b\right\}.$$

Let $\phi^*(x | \mathbf{x})$ be the density of X conditional on $\dot{\mathbf{X}} = \mathbf{x}$. Then conditioning on $\dot{\mathbf{X}} = \mathbf{x}$ and approximating the distribution function of X as a linear function about b , we have

$$\begin{aligned} &P\left(X \geq b - \max_{\mathbf{s} \in \partial C} (\mathbf{s} - \mathbf{t})'\mathbf{x} \mid \dot{\mathbf{X}} = \mathbf{x}\right) \\ &\approx P(X \geq b \mid \dot{\mathbf{X}} = \mathbf{x}) + \max_{\mathbf{s} \in \partial C} (\mathbf{s} - \mathbf{t})'\mathbf{x} \phi^*(b | \mathbf{x}). \end{aligned}$$

Taking expectations over $\dot{\mathbf{X}}$ and reversing the order of conditioning, we have

$$E\{\chi_{\text{HA}}(b)\} \approx P(X \geq b) + E\left\{\max_{\mathbf{s} \in \partial C} (\mathbf{s} - \mathbf{t})' \dot{\mathbf{X}} \mid X = b\right\} \phi_0(b).$$

Now let $\dot{\mathbf{X}} = r\mathbf{u}$, where $r = \|\dot{\mathbf{X}}\|$ and \mathbf{u} is a unit vector. Because $X(\mathbf{t})$ is isotropic, \mathbf{u} is uniformly distributed on the surface of the unit N -sphere independent of r . Thus $\max_{\mathbf{s} \in \partial C} (\mathbf{s} - \mathbf{t})' \dot{\mathbf{X}}$ is just r times the maximum perpendicular distance of ∂C from \mathbf{t} projected onto \mathbf{u} ; averaged over all \mathbf{u} , this becomes r times half the average caliper diameter of C , or $r\Delta(C)/2$. Thus

$$E\left\{\max_{\mathbf{s} \in \partial C} (\mathbf{s} - \mathbf{t})' \dot{\mathbf{X}} \mid X = b\right\} = \Delta(C) E(r \mid X = b)/2.$$

Combining these results, we obtain

$$E\{\chi_{\text{HA}}(b)\} \approx \Delta(C) E(r \mid X = b) \phi_0(b)/2 + P(X \geq b).$$

In two dimensions an elementary result of integral geometry states that the mean caliper diameter of a piecewise smooth convex set equals the perimeter length divided by π , $\Delta(C) = |\partial C|/\pi$ [see Santaló (1976), page 30]. Combining this with (3.2) we get

$$E\{\chi_{\text{HA}}(b)\} \approx |\partial C| \rho_1(b)/2 + P(X \geq b),$$

which agrees with the last two terms of the result of Theorem 2. In three dimensions it can be shown that $\Delta(C) = H(\partial C)/(2\pi)$ [see Santaló (1976), page 226]. Combining this with (A.6) we get

$$E\{\chi_{\text{HA}}(b)\} \approx H(\partial C) \rho_1(b)/\pi + P(X \geq b),$$

which agrees with the last two terms of the result of Theorem 3.

This agreement suggests that the expected Hadwiger characteristic can serve as a good approximation for the exceedence probability of the maximum of an isotropic random field above high thresholds in a small convex set. This is of particular interest in the medical applications described in the next section, where C is often restricted to a small part of the brain such as the left temporal lobe. This approximation is related to work by Knowles and Siegmund (1989) and Sun (1993).

6. Applications.

6.1. *Approximating the Hadwiger characteristic from a finite sampling of $X(\mathbf{t})$.* In practice random fields are sampled on a square lattice of pixels in two dimensions, or a cubic lattice of voxels in three dimensions. If the set C is an interval, Adler [(1977) and (1981), page 117] gives a method based on Serra (1969) of approximating the IG characteristic in two and three dimensions. It is straightforward to show that the Hadwiger characteristic can be approximated in a similar way, as follows. In two dimensions, suppose $C = I$ and the lattice points are $l_{ij} = (i/M, j/M)$, $i, j = 0, \dots, M$. Let P_M be the number of lattice points inside the excursion set A_b , let E_M be the number of

edges joining two adjacent lattice points l_{ij} and $l_{i+1,j}$, or l_{ij} and $l_{i,j+1}$, both of whose end points are in A_b , and let F_M be the number of faces of four adjacent lattice points $l_{ij}, l_{i+1,j}, l_{i,j+1}$ and $l_{i+1,j+1}$, all of which are inside A_b . Following the proof of Adler [(1981), Theorem 5.5.1] it is straightforward to show that for a random field in two dimensions satisfying the regularity conditions of Theorem 1,

$$\chi_{\text{HA}}(b) = \lim_{M \rightarrow \infty} P_M - E_M + F_M,$$

with probability 1.

For three dimensions, suppose $C = I$ and the lattice points are $l_{ijk} = (i/M, j/M, k/M)$, $i, j, k = 0, \dots, M$. Let P_M be the number of lattice points inside the excursion set A_b , let E_M be the number of edges joining two adjacent lattice points $\{l_{ijk}, l_{i+1,j,k}\}$, $\{l_{ijk}, l_{i,j+1,k}\}$ or $\{l_{ijk}, l_{i,j,k+1}\}$, both of whose end points are in A_b , let F_M be the number of faces of four adjacent lattice points $\{l_{ijk}, l_{i+1,j,k}, l_{i,j+1,k}, l_{i+1,j,k+1}\}$, $\{l_{ijk}, l_{i+1,j,k}, l_{i,j,k+1}, l_{i+1,j,k+1}\}$ or $\{l_{ijk}, l_{i,j+1,k}, l_{i,j,k+1}, l_{i,j+1,k+1}\}$, all of which are inside A_b , and let Q_M be the number of cubes $\{l_{ijk}, l_{i+1,j,k}, l_{i,j+1,k}, l_{i+1,j+1,k}, l_{i,j,k+1}, l_{i+1,j,k+1}, l_{i,j+1,k+1}, l_{i+1,j+1,k+1}\}$, all of whose vertices are in A_b . Then for a random field in three dimensions satisfying the regularity conditions of Theorem 1,

$$\chi_{\text{HA}}(b) = \lim_{M \rightarrow \infty} P_M - E_M + F_M - Q_M,$$

with probability 1.

Three-dimensional sets C that have piecewise smooth boundaries can be tessellated with a finite number of components, all of which are bounded by a ball of radius ε for any $\varepsilon > 0$ in such a way that tangent planes of the tessellation approach those of C as $\varepsilon \rightarrow 0$. Let $P_\varepsilon, E_\varepsilon, F_\varepsilon$ and Q_ε be the number of points, edges, faces and components of the tessellation contained in A_b . Then extending the above arguments, it can be shown that for a random field satisfying the regularity conditions of Theorem 1,

$$\chi_{\text{HA}}(b) = \lim_{\varepsilon \rightarrow 0} P_\varepsilon - E_\varepsilon + F_\varepsilon - Q_\varepsilon,$$

with probability 1, with the obvious extension to a tiling in two dimensions.

In practice, it is a difficult programming task to carry out such a tessellation in three dimensions working with data sampled on a cubic lattice. One possibility is to choose the components as the cubes entirely contained in C together with truncated cubes, with faces suitably triangulated, whose vertices touch the boundary of C . Another possibility, which we shall use in the example in the next section, is to simply drop all cubes that touch the boundary of C and let \tilde{C} be the union of all cubes entirely contained in C . Although the volume of \tilde{C} approximates the volume of C , \tilde{C} is not very satisfactory, since now the tangent planes of \tilde{C} do not approximate those of C , but it is very easy to work with. The expectation of $\chi_{\text{HA}}(b)$ inside \tilde{C} for a suitably regular isotropic field can be calculated as follows. Let \tilde{P} be the number of points in \tilde{C} , let \tilde{E}_1, \tilde{E}_2 and \tilde{E}_3 be the number of edges in \tilde{C} in the t_1, t_2 and t_3 directions, respectively, let $\tilde{F}_{23}, \tilde{F}_{31}$ and \tilde{F}_{12} be the number of

faces in \tilde{C} normal to the t_1 , t_2 and t_3 directions, respectively, and let \tilde{Q} be the number of cubes in \tilde{C} . Finally, let δ_1 , δ_2 and δ_3 be the separation between adjacent voxels in the directions t_1 , t_2 and t_3 . Generalising (4.2), it can be shown that

$$\begin{aligned} |\tilde{C}| &= \tilde{Q} \delta_1 \delta_2 \delta_3, \\ |\partial\tilde{C}|/2 &= (\tilde{F}_{12} - \tilde{Q}) \delta_1 \delta_2 + (\tilde{F}_{31} - \tilde{Q}) \delta_3 \delta_1 + (\tilde{F}_{23} - \tilde{Q}) \delta_2 \delta_3, \\ H(\partial\tilde{C})/\pi &= (\tilde{E}_1 - \tilde{F}_{12} - \tilde{F}_{31} + \tilde{Q}) \delta_1 + (\tilde{E}_2 - \tilde{F}_{12} - \tilde{F}_{23} + \tilde{Q}) \delta_2 \\ &\quad + (\tilde{E}_3 - \tilde{F}_{31} - \tilde{F}_{23} + \tilde{Q}) \delta_3, \\ \psi(\tilde{C}) &= \tilde{P} - (\tilde{E}_1 + \tilde{E}_2 + \tilde{E}_3) + (\tilde{F}_{23} + \tilde{F}_{31} + \tilde{F}_{12}) - \tilde{Q}. \end{aligned}$$

Substituting these in Theorem 3 gives the desired expectation.

The observed Hadwiger characteristic of the excursion set in \tilde{C} can be approximated by $P - E + F - Q$, where P , E , F and Q are the numbers of points, edges, faces and cubes, respectively, of \tilde{C} entirely contained in the excursion set. For a large number of thresholds, these calculations can be performed very rapidly by cumulating P , E , F and Q in parallel with one pass through the data. The computer program used in the following subsections takes the values of $X(\mathbf{t})$ at eight adjacent voxels and first determines their range. Obviously there will be no cumulative contributions to $\chi_{\text{HA}}(b)$ from thresholds b outside the range of the eight values, and so contributions are cumulated only for thresholds within the range. At the same time, the program determines the volume, surface area, mean curvature and Hadwiger characteristic of \tilde{C} as defined above. Memory usage is negligible since only a small portion of the data is needed at any one time. This makes it possible to find the Hadwiger characteristic for a 1.3 million voxel three-dimensional field at 1000 thresholds in a few minutes on a typical workstation.

6.2. *Gaussian random fields with a Gaussian correlation function.* Worsley, Evans, Marrett and Neelin (1992, 1993) modelled the noise in PET images in \mathbb{R}^3 as a white noise Gaussian random field convolved with a kernel or "point response function" proportional to $\exp(-\mathbf{h}'\Sigma^{-1}\mathbf{h}/2)$, where \mathbf{h} is a vector in \mathbb{R}^3 , $\Sigma = \text{diag}(\sigma_1^2, \sigma_2^2, \sigma_3^2)$ is a 3×3 diagonal matrix that governs the width of the kernel and the prime denotes transpose. The width of the kernel is usually measured in terms of the full width at half maximum, or the width of the kernel at half its maximum value. If F_1 , F_2 and F_3 are the full width at half maxima in each of the three dimensions, then by equating $\exp[-(F_j/2)^2/(2\sigma_j^2)]$ to $1/2$, we obtain $\sigma_j = (8 \log_e 2)^{-1/2} F_j$. Rescaling the image by dividing the j th coordinate by $(4 \log_e 2)^{-1/2} F_j$ gives an isotropic point response function and thus an isotropic Gaussian random field $X(\mathbf{t})$ with Gaussian correlation function $R(\mathbf{h}) = \exp(-\|\mathbf{h}\|^2/2)$. Such a field satisfies the conditions of Theorem 1, Λ is the identity matrix and $\det(\Lambda) = 1$.

6.3. *Application to the study of pain perception.* Talbot, Marrett, Evans, Meyer, Bushnell and Duncan (1991) carried out an experiment in which PET cerebral blood flow images were obtained for eight subjects while a thermistor was applied to the forearm at both warm (42°C) and hot (48°C) temperatures, each condition being studied twice on each subject. The purpose of the experiment was to find regions of the brain that were activated by the hot stimulus, compared to the warm stimulus. For the present work, we shall analyse the difference images of the two warm conditions as a data set which should have an expectation of zero throughout. The difference images were reconstructed to a resolution of $F_1 = 20$ mm, $F_2 = 20$ mm and $F_3 = 7.6$ mm, then aligned and sampled on a $128 \times 128 \times 80$ lattice of voxels, separated at approximately $d_1 = 1.4$ mm, $d_2 = 1.7$ mm and $d_3 = 1.5$ mm on the front-back, left-right and vertical axes, respectively. Rescaling the coordinates to produce an isotropic field gives $\delta_j = (4 \log_e 2)^{1/2} (d_j / F_j)$, $j = 1, 2, 3$. These images were averaged and divided by a pooled estimate of their standard deviation to produce an image $X(\mathbf{t})$ that was modelled as a zero mean, unit variance, isotropic stationary Gaussian random field with a Gaussian correlation function $R(\mathbf{h})$ [see Worsley, Evans, Marrett and Neelin (1992, 1993)].

The region of the brain \tilde{C} of interest occupied a volume of $|\tilde{C}| = 1564$, with surface area $|\partial\tilde{C}| = 979$, mean curvature $H(\partial\tilde{C}) = 137$ and Hadwiger characteristic $\psi(\tilde{C}) = 1$ calculated from Section 6.1 (see Figure 1(a)). The expected Hadwiger characteristic from Theorem 3 and (2.3) was plotted against the threshold b in Figure 5(a), together with the observed Hadwiger characteristic approximated as at the end of Section 6.1. Also shown for comparison is the AIG characteristic and its expected value, which equals the first term $|\tilde{C}| \rho_3(b)$ of Theorem 3 [Worsley, Evans, Marrett and Neelin (1992)]. The agreement between observed and expected seems reasonable, and both characteristics are very close for excursion sets above high thresholds [Figure 5(b)]. The number of regions of activation was estimated using the method of Worsley, Evans, Marrett and Neelin (1993). For a nominal bias of $\alpha = 0.1$, the value b_α chosen so that $E\{\chi_{\text{HA}}(b_\alpha)\} = \alpha$ was $b_\alpha = 4.24$. The observed Hadwiger characteristic at this threshold was $\chi_{\text{HA}}(b_\alpha) = 0$, indicating no regions of activation, as predicted. The same result was obtained with the AIG characteristic.

6.4. *Application to the word recognition study.* D. Bub (private communication, 1992) carried out an experiment in which PET cerebral blood flow data were collected from 10 normal volunteers. Visual stimuli were presented for 1 s with an interstimulus interval of 1 s on a monochrome monitor, suspended in front of the subject and covered by a light-tight curtain. The baseline condition was a black plus sign on a white background and for the activation condition, single words were presented on the monitor for 1 s with an interstimulus interval of 1 s. The same methodology as for the pain study was repeated. The region of the brain \tilde{C} of interest occupied a volume of $|\tilde{C}| = 997$, with $|\partial\tilde{C}| = 2318$, $H(\partial\tilde{C}) = 93$ and $\psi(\tilde{C}) = -3$, since in this case

\tilde{C} contained several “holes” in the thin shell chosen as the search volume (see Figure 1(b)). Note also that the surface area is large and the mean curvature is small, since \tilde{C} is a thin shell.

Figure 5(c) plots the same information as in Figure 5(a), but this time there are substantial discrepancies between observed and expected Hadwiger characteristic, particularly for high threshold values as shown in Figure 5(d), which can be attributed to peaks or regions of activation due to the word recognition task. We can estimate the number of peaks by the method of Worsley, Evans, Marrett and Neelin (1993). For a nominal bias of $\alpha = 0.1$, the value b_α chosen so that $E\{\chi_{\text{HA}}(b_\alpha)\} = \alpha$ was $b_\alpha = 4.22$. The observed Hadwiger characteristic at this threshold was $\chi_{\text{HA}}(b_\alpha) = 3$, indicating three

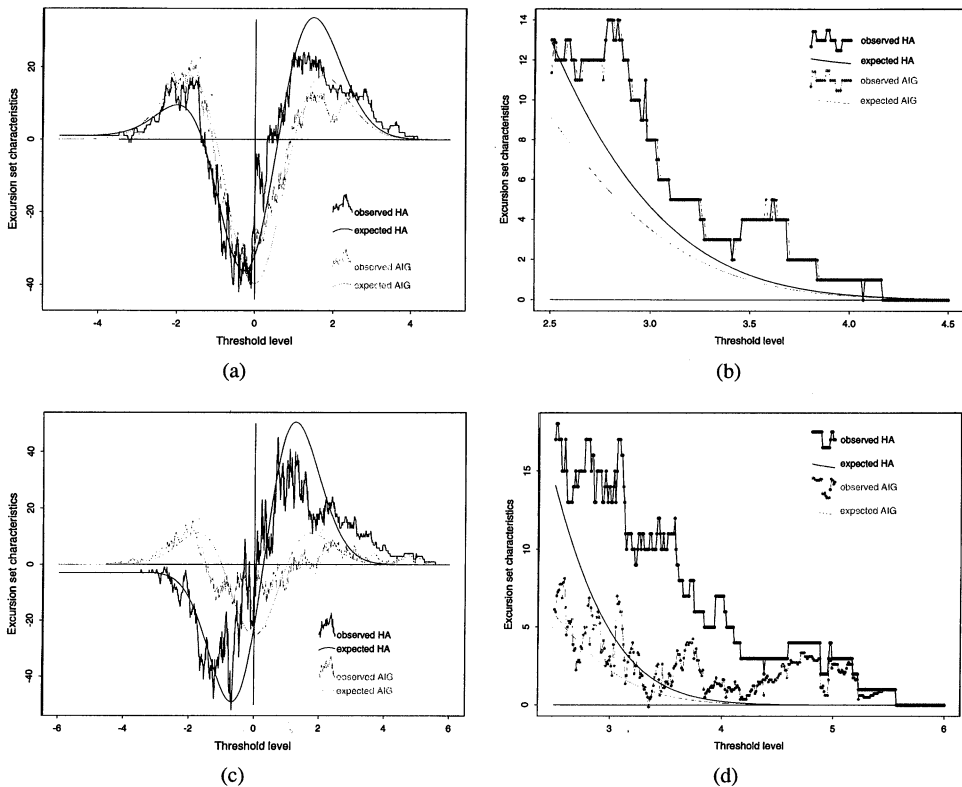


FIG. 5. Application of the excursion set characteristics to the data sets. The observed Hadwiger characteristic for $X(t)$ (jagged line) and its expectation (smoothed line) are plotted against the threshold b for (a) the pain study and (c) the word recognition study, together with the AIG characteristic (shaded lines). Parts (b) and (d) show the upper tails of (a) and (c), respectively. For the pain study the observed characteristic is close to the expected characteristic, indicating no evidence of increased activation. For the word recognition study the observed Hadwiger characteristic is approximately three units larger than expected in the upper tail ($4 < b < 5$), indicating evidence of at least three regions of activation. The AIG characteristic, on the other hand, indicates only one region of activation.

regions of activation. These were identified by Worsley, Evans, Marrett and Neelin (1992) in the extrastriate, left temporal and left frontal. The regions are shown in Figure 1(b) close to $\mathbf{t} = (-2.8, -6.7, -0.9)$ cm, $\mathbf{t} = (-5.8, -0.3, -0.9)$ cm and $\mathbf{t} = (-4.7, 4.3, 0.3)$ cm, respectively. The observed AIG characteristic at the $\alpha = 0.1$ threshold of 4.07 is 1.125. Since the excursion set touches the boundary of \tilde{C} , the AIG characteristic picks up only one of the three regions of activation. This example clearly shows the superiority of the Hadwiger characteristic when the regions of activation are close to the boundary of \tilde{C} .

APPENDIX

A.1. *Proof of Lemma 6.* We evaluate the expectation in Lemma 4 by changing to polar coordinates. Let $X_{\perp} = r \cos \alpha$ and $X_3 = r \sin \alpha$, $r \geq 0$, $0 \leq \alpha < 2\pi$, so that we can write $X_U = X_{\perp} \cos \theta + X_3 \sin \theta = r \cos(\alpha - \theta)$. Since the field is isotropic and X_T, X_{\perp} and X_3 are derivatives of X in orthogonal directions, then α is uniformly distributed on $[0, 2\pi)$ independent of r or X_{TT} , conditional on $X = b$ and $X_T = 0$. Taking expectations over α conditional on $X = b$ and $X_T = 0$, we have

$$\begin{aligned} & E\{(X_{\perp} < 0)X_U^+(X_{TT} + c_{TT}X_{\perp})\} \\ (A.1) \quad & = E\{(\cos \alpha < 0)r \cos(\alpha - \theta) [\cos(\alpha - \theta) > 0](X_{TT} + c_{TT}r \cos \alpha)\} \\ & = E(rX_{TT})(1 - \cos \theta)/(2\pi) - E(r^2)c_{TT}(\sin \theta - \theta \cos \theta)/(4\pi). \end{aligned}$$

We start with the first term of (A.1). Converting back from polar coordinates, we have, conditional on $X = b$ and $X_T = 0$,

$$(A.2) \quad E(rX_{TT}) = \pi E\left\{r \int_0^{\pi} \sin \alpha \, d\alpha / (2\pi) X_{TT}\right\} = \pi E(X_3^+ X_{TT}),$$

and since $X(\mathbf{t})$ is isotropic,

$$(A.3) \quad E(X_3^+ X_{TT} | X = b, X_T = 0) \phi_T(b, 0) = -\rho_2(b).$$

We now tackle the second term of (A.1). Since $X(\mathbf{t})$ is isotropic, we can write the joint density of (X_T, X_{\perp}) conditional on $X = x$ at (x_T, x_{\perp}) as $f(x_T^2 + x_{\perp}^2)$ for some function f . Note that f is not a density function. Then

$$(A.4) \quad E(X_{\perp}^2 | X = b, X_T = 0) \phi_T(b, 0) = \int_{-\infty}^{\infty} x_{\perp}^2 f(x_{\perp}^2) \, dx_{\perp} \phi_0(b).$$

Now converting to polar coordinates $X_T = y \cos \omega$ and $X_{\perp} = y \sin \omega$ for $y \geq 0$ and $0 \leq \omega < 2\pi$, we have

$$E(X_{\perp}^+ | X = b) = \int_{-\infty}^{\infty} \int_{-\infty}^{\infty} x_{\perp}^+ f(x_T^2 + x_{\perp}^2) \, dx_T \, dx_{\perp} = 2 \int_0^{\infty} y^2 f(y^2) \, dy.$$

Combining this with (A.4) applied to X_3 as well as X_{\perp} and noting that

$r^2 = X_{\perp}^2 + X_3^2$, we have

$$(A.5) \quad \begin{aligned} E(r^2 | X = b, X_T = 0) \phi_T(b, 0) \\ = 2E(X_{\perp}^+ | X = b) \phi_0(b) = 2\rho_1(b). \end{aligned}$$

Putting together (A.1), (A.2), (A.3) and (A.5), we have

$$\begin{aligned} -E\{(X_{\perp} < 0) X_U^+(X_{TT} + c_{TT} X_{\perp}) | X = b, X_T = 0\} \phi_T(b, 0) \\ = \rho_2(b)(1 - \cos \theta)/2 + \rho_1(b)c_{TT}(\sin \theta - \theta \cos \theta)/(2\pi). \end{aligned}$$

We obtain the final result by integrating over the surface of ∂C and using

$$\iint_{\partial C_S} (1 - \cos \theta) dt_T dt_U = |\partial C|. \quad \square$$

A.2. Proof of Lemma 7. We start with the case where $\partial C \cap \mathcal{E}_u$ is convex at \mathbf{t} and we evaluate the expectation of the first term in Lemma 5 by changing to polar coordinates. Let $X_1 = r \cos \alpha \sin \beta$, $X_2 = r \sin \alpha \sin \beta$ and $X_3 = r \cos \beta$, $r \geq 0$, $0 \leq \alpha < 2\pi$ and $0 \leq \beta \leq \pi$. Let θ be the angle between the edge ∂C_E in the positive (upward) direction of t_3 and the plane \mathcal{E}_u at $\mathbf{t} = (t_1, t_2, u)$. Then for some $0 \leq \alpha_1 < 2\pi$, $0 \leq \alpha_2 < 2\pi$, $0 \leq \alpha_E < 2\pi$, $0 \leq \theta \leq \pi$, we can write $X_{Tj} = X_1 \cos \alpha_j + X_2 \sin \alpha_j = r \cos(\alpha - \alpha_j) \sin \beta$, $j = 1, 2$, and $X_E = r\{\cos(\alpha - \alpha_E) \sin \beta \cos \theta + \cos \beta \sin \theta\}$. Since the field is isotropic, then r , α and β are independent random variables conditional on X ; α is uniformly distributed on $[0, 2\pi)$ and the density of β is $(\sin \beta)/2$ on $[0, \pi]$. Then since $r \geq 0$, $\sin \beta \geq 0$ and $\sin \theta \geq 0$,

$$\begin{aligned} E\{(X_{T1} < 0)(X_{T2} < 0) X_E^+ | X\} \\ = E\{[\cos(\alpha - \alpha_1) < 0][\cos(\alpha - \alpha_2) < 0] \\ \times r[\cos(\alpha - \alpha_E) \sin \beta \cos \theta + \cos \beta \sin \theta] \\ \times [\cot \beta > -\cos(\alpha - \alpha_E) \cot \theta] | X\} \\ = E(r | X) E\{[\cos(\alpha - \alpha_1) < 0][\cos(\alpha - \alpha_2) < 0] \sin \theta (1 - \gamma \cot \gamma)\} / 4, \end{aligned}$$

where $\gamma = \cot^{-1}[-\cos(\alpha - \alpha_E) \cot \theta]$, $0 \leq \gamma \leq \pi$. Converting back from polar coordinates, we have

$$(A.6) \quad \begin{aligned} E(r | X) &= 4E\left(r \int_0^{\pi/2} \cos \beta \sin \beta d\beta / 2 | X\right) \\ &= 4E\{(r \cos \beta)^+ | X\} = 4E(X_3^+ | X). \end{aligned}$$

Because the edge is convex, we can assume without loss of generality that $0 \leq \alpha_2 - \alpha_1 \leq \pi$, so that

$$[\cos(\alpha - \alpha_1) < 0][\cos(\alpha - \alpha_2) < 0] = (\pi/2 + \alpha_2 < \alpha < 3\pi/2 + \alpha_1).$$

Then taking expectations over α , we have

$$\begin{aligned} & 2\pi E\{[\cos(\alpha - \alpha_1) < 0][\cos(\alpha - \alpha_2) < 0]\sin\theta(1 - \gamma \cot\gamma)\} \\ &= \int_{\pi/2 + \alpha_2}^{3\pi/2 + \alpha_1} \sin\theta(1 - \gamma \cot\gamma) d\alpha \\ &= \tan^{-1}\left(\frac{\tan(\alpha_1 - \alpha_E)}{\sin\theta}\right) - \cos(\alpha_1 - \alpha_E)\cos\theta \tan^{-1}\left(-\frac{\tan\theta}{\sin(\alpha_1 - \alpha_E)}\right) \\ &\quad + \pi - \tan^{-1}\left(\frac{\tan(\alpha_2 - \alpha_E)}{\sin\theta}\right) \\ &\quad - \cos(\alpha_2 - \alpha_E)\cos\theta \tan^{-1}\left(\frac{\tan\theta}{\sin(\alpha_1 - \alpha_E)}\right). \end{aligned}$$

Using standard Euclidean geometry it can be shown that, for $j = 1, 2$,

$$\cos\omega_j = \cos(\alpha_j - \alpha_E)\cos\theta, \quad \tan\theta_j = \frac{(-1)^j \tan\theta}{\sin(\alpha_2 - \alpha_E)}$$

and

$$\delta = \tan^{-1}\left(\frac{\tan(\alpha_1 - \alpha_E)}{\sin\theta}\right) - \tan^{-1}\left(\frac{\tan(\alpha_2 - \alpha_E)}{\sin\theta}\right).$$

Combining these results, we obtain

$$\begin{aligned} & E\{(X_{T_1} < 0)(X_{T_2} < 0)X_E^+ | X = b\}\phi_0(b) \\ &= (\pi - \delta - \theta_1 \cos\omega_1 - \theta_2 \cos\omega_2)\rho_1(b)/(2\pi). \end{aligned}$$

Similar arguments for the concave case show that

$$\begin{aligned} & E\{(X_{T_1} > 0)(X_{T_2} > 0)X_E^+ | X = b\}\phi_0(b) \\ &= -(\pi - \delta - \theta_1 \cos\omega_1 - \theta_2 \cos\omega_2)\rho_1(b)/(2\pi), \end{aligned}$$

and combining these two results proves the lemma. \square

A.3. Proof of Lemma 8. Let c_T be the curvature of S in the direction of \mathbf{t}_T and let c_U be the curvature of S in the direction of \mathbf{t}_U . Since \mathbf{t}_U is inclined at an angle θ to \mathcal{E}_u , then $c_T = c_{TT} \sin\theta$ and, by the Frenet formula, $c_U = -d\theta/d\mathbf{t}_U$. Since the sum of curvatures in orthogonal directions is invariant under rotation, we have

$$c_{\max} + c_{\min} = c_T + c_U = c_{TT} \sin\theta - d\theta/d\mathbf{t}_U.$$

Substituting this into the first term of the right-hand side of the lemma, we have

$$\begin{aligned} & \iint_S c_{TT}(\sin\theta - \theta \cos\theta) d\mathbf{t}_T d\mathbf{t}_U \\ (A.7) \quad &= \iint_S (c_{\max} + c_{\min}) d\mathbf{t}_T d\mathbf{t}_U + \iint_S \left(\frac{d\theta}{d\mathbf{t}_U} - c_{TT}\theta \cos\theta\right) d\mathbf{t}_T d\mathbf{t}_U. \end{aligned}$$

It remains to show that the second term of the right-hand side of (A.7) cancels with the line integral of the second term of the left-hand side of the lemma. To do this, define the vector field $\mathbf{F} = \theta \mathbf{t}_T$ so that $\mathbf{F} \cdot \mathbf{r} = \theta \cos \omega$ and so by Stokes's theorem,

$$(A.8) \quad \int_{\partial S} \theta \cos \omega \, d\mathbf{r} = \oint_{\partial S} \mathbf{F} \cdot \mathbf{r} \, d\mathbf{r} = \iint_S \text{curl } \mathbf{F} \cdot \mathbf{N} \, dt_T \, dt_U,$$

where \mathbf{N} is the unit outside normal to S . Let t_T and t_U be coordinates with respect to axes \mathbf{t}_T and \mathbf{t}_U and origin at \mathbf{t} on S . Then $d\mathbf{F}/dt_U = (d\theta/dt_U)\mathbf{t}_T$ and, by the Frenet formula, $d\mathbf{F}/dt_T = c_{TT}\theta\mathbf{t}_\perp$, where as before \mathbf{t}_\perp was the unit inside normal to $S \cap \mathcal{E}_u$. Since \mathbf{t}_U is inclined at angle θ to \mathbf{t}_\perp , then

$$(A.9) \quad \text{curl } \mathbf{F} \cdot \mathbf{N} = \frac{d\mathbf{F}}{dt_U} \cdot \mathbf{t}_T - \frac{d\mathbf{F}}{dt_T} \cdot \mathbf{t}_U = \frac{d\theta}{dt_U} - c_{TT}\theta \cos \theta.$$

Combining (A.7), (A.8) and (A.9) gives the result. \square

Acknowledgments. The author would like to acknowledge the encouragement and assistance of A. C. Evans, S. Marrett and P. Neelin of the Brain Imaging Centre of the Montreal Neurological Institute. The author would like to thank Dr. D. Bub, Dr. C. Bushnell and Dr. G. Duncan for permission to use their data, W. Jonsson for help with the proof of Lemma 8, and the referee for a careful and helpful reading of the paper.

REFERENCES

- ADLER, R. J. (1977). A spectral moment estimator in two dimensions. *Biometrika* **64** 367–373.
 ADLER, R. J. (1981). *The Geometry of Random Fields*. Wiley, New York.
 ADLER, R. J. and HASOFER, A. M. (1976). Level crossings for random fields. *Ann. Probab.* **4** 1–12.
 GOTT, J. R., MELOTT, A. L. and DICKINSON, M. (1986). The sponge-like topology of large-scale structure in the universe. *Astrophys. J.* **306** 341–357.
 GOTT, J. R., PARK, C., JUSZKIEWICZ, R., BIES, W. E., BENNETT, D. P., BOUCHET, F. R. and STEBBINS, A. (1990). Topology of microwave background fluctuations: theory. *Astrophys. J.* **352** 1–14.
 HADWIGER, H. (1959). Normale Körper in euklidischen Raum und ihre topologischen und metrischen Eigenschaften. *Math. Z.* **71** 124–140.
 HASOFER, A. M. (1978). Upcrossings of random fields. *Adv. in Appl. Probab. (Suppl.)* **10** 14–21.
 KNOWLES, M. and SIEGMUND, D. (1989). On Hotelling's approach to testing for a nonlinear parameter in regression. *Internat. Statist. Rev.* **57** 205–220.
 KNUTH, D. E. (1992). Two notes on notation. *Amer. Math. Monthly* **99** 403–422.
 RHOADS, J. E., GOTT, J. R. and POSTMAN, M. (1994). The genus curve of the Abell clusters. *Astrophys. J.* **421** 1–8.
 SANTALÓ, L. A. (1976). *Integral Geometry and Geometric Probability. Encyclopedia of Mathematics and its Applications 1*. Addison-Wesley, Reading, MA.
 SERRA, J. (1969). Introduction à la morphologie mathématique. *Cahiers du Centre de Morphologie Mathématique* **3**. Ecole des Mines, Paris.
 SIEGMUND, D. O. and WORSLEY, K. J. (1995). Testing for a signal with unknown location and scale in a stationary Gaussian random field. *Ann. Statist.* **23** 608–639.
 SMOOT, G. F., BENNETT, C. L., KOGUT, A., WRIGHT, E. L., AYMONT, J., BOGGESS, N. W., CHENG, E. S., DE AMICI, G., GULKIS, S., HAUSER, M. G., HINSHAW, G., JACKSON, P. D., JANSSEN, M., KAITA, E., KELSALL, T., KEEGSTRA, P., LINEWEAVER, C., LOWENSTEIN, K., LUBIN, P.,

- MATHER, J., MEYER, S. S., MOSELEY, S. H., MURDOCK, T., ROKKE, L., SILVERBERG, R. F., TENORIO, L., WEISS, R. and WILKINSON, D. T. (1992). Structure in the COBE differential microwave radiometer first-year maps. *Astrophys. J.* **396** L1–L5.
- SUN, J. (1993). Tail probabilities of the maxima of Gaussian random fields. *Ann. Probab.* **21** 34–71.
- TALBOT, J. D., MARRETT, S., EVANS, A. C., MEYER, E., BUSHNELL, M. C. and DUNCAN, G. H. (1991). Multiple representations of pain in human cerebral cortex. *Science* **251** 1355–1358.
- TORRES, S. (1994). Topological analysis of COBE-DMR cosmic microwave background maps. *Astrophys. J.* **423** L9–L12.
- WORSLEY, K. J. (1994a). Local maxima and the expected Euler characteristic of excursion sets of χ^2 , F , and t fields. *Adv. in Appl. Probab.* **26** 13–42.
- WORSLEY, K. J. (1994b). Boundary corrections for the expected Euler characteristic of excursion sets of random fields, with an application to astrophysics. *Adv. in Appl. Probab.* To appear.
- WORSLEY, K. J., EVANS, A. C., MARRETT, S. and NEELIN, P. (1992). A three dimensional statistical analysis for CBF activation studies in human brain. *Journal of Cerebral Blood Flow and Metabolism* **12** 900–918.
- WORSLEY, K. J., EVANS, A. C., MARRETT, S. and NEELIN, P. (1993). Detecting changes in random fields and applications to medical images. Unpublished manuscript.

DEPARTMENT OF MATHEMATICS AND STATISTICS
MCGILL UNIVERSITY
805 OUEST, RUE SHERBROOKE
MONTRÉAL, QUÉBEC
CANADA H3A 2K6

